

## 19.5. Fibre diffraction

BY R. CHANDRASEKARAN AND G. STUBBS

### 19.5.1. Introduction

Many biopolymers are long helical structures and have a natural tendency to form fibres. This tendency severely impedes the growth of single crystals from these polymers, and even if crystals can be grown, the molecular interactions in the crystals rarely correspond to the biologically significant interactions in the fibres. Conventional macromolecular crystallography is therefore often not applicable to these systems. Fibre diffraction, however, is a powerful technique for determining the structural details of such polymers. It has been used to study a wide variety of biopolymers, ranging from simple polypeptides, polynucleotides and polysaccharides to complex filamentous viruses and cytoskeletal filaments.

Fibres can have relatively high degrees of order, although falling short of true three-dimensional crystallinity. The key difference between fibres and crystals, however, is that in fibres the fundamental structural aggregates, although parallel to each other, are randomly oriented about the fibre axis. Consequently, the diffraction pattern is cylindrically averaged. This cylindrical averaging is the defining characteristic of fibre diffraction.

On the basis of this definition, fibre diffraction may also be considered to include diffraction from many biological membrane specimens, and much of fibre-diffraction theory also applies to membrane diffraction. In general, however, the diffracting units in fibres have helical symmetry, whereas those of membranes do not.

In addition to the loss of information due to cylindrical averaging, fibre-diffraction patterns reflect a generally limited degree of order and rarely extend beyond 3 Å resolution. Consequently, the number of data obtainable from a fibre is considerably less than that from a single crystal having a similar size of asymmetric unit. The use of stereochemical information to supplement the diffraction data is therefore essential. For polymers with small asymmetric units, such as polynucleotides, structural chemical information can be used to construct models consistent with the helical parameters and molecular dimensions obtained from the diffraction data. For the larger asymmetric units found in aggregates, such as viruses, initial models must be constructed in other ways. However, in all cases the combination of diffraction data and stereochemistry can be used to refine both molecular structures and packing parameters. Refinement in this way is very similar to that used in macromolecular crystallography, but because of the limited number of experimental data, stereochemical restraints are particularly important in fibre diffraction. As in crystallography, difference-electron-density maps are used in conjunction with refinement to identify missing portions and determine the correctness of the models and, in favourable cases, to locate ions and solvent molecules associated with the polymers.

### 19.5.2. Types of fibres

Fibres fall into essentially two classes with respect to the degree of ordering of the polymer chains. Within each class, there are varying degrees of disorder; furthermore, many fibres exhibit properties intermediate between those of the two ideal classes.

In noncrystalline fibres, the polymers are parallel to each other, but their positions and orientations are otherwise uncorrelated. Diffraction patterns from these fibres are confined to layer lines (Fig. 19.5.2.1*a*) because of the repeating nature of the polymer helix, but are otherwise continuous and correspond to the cylindrical average of the Fourier transform of a single particle.

In polycrystalline fibres, the polymers form fully ordered microcrystallites, and each fibre consists of many such micro-

crystallites, randomly oriented about the fibre axis. In diffraction patterns from polycrystalline fibres, the layer lines are sampled to form discrete reflections (Fig. 19.5.2.1*b*); the diffraction pattern is the cylindrical average of a single-crystal diffraction pattern and is, in fact, equivalent to the diffraction pattern that would be obtained from a rotating single crystal.

Polycrystalline fibres may be disordered in various ways. For example, the helical polymers may be subject to rotational or translational disorder, and this disorder may be partial (a small number of alternative packings for each particle) or complete (for example, completely random rotational particle orientations). Rotational disorder may be coupled to translational disorder (screw disorder). The resulting diffraction patterns may contain both discrete reflections and continuous diffraction along layer lines; depending upon the type of disorder, the discrete reflections

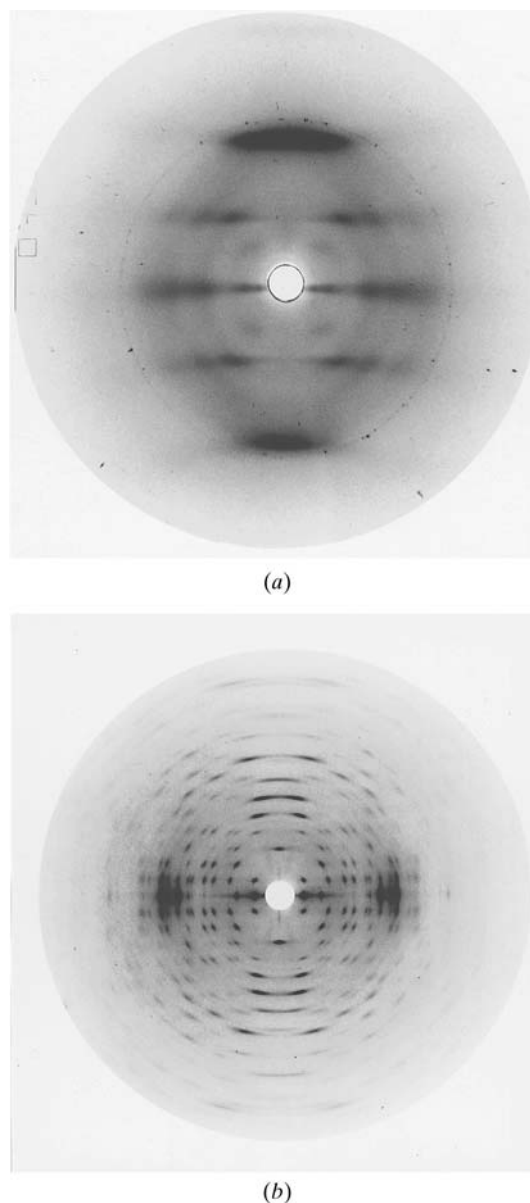


Fig. 19.5.2.1. X-ray diffraction patterns showing (a) continuous intensity on layer lines from an oriented nucleic acid fibre and (b) Bragg reflections from an oriented and polycrystalline polysaccharide fibre.

## 19.5. FIBRE DIFFRACTION

may be confined to the equator (layer line zero) or the low-resolution part of the pattern, or they may be dispersed throughout the pattern. Variations in diffraction effects due to different types of disorder have been discussed by Arnott (1980) and Stroud & Millane (1995).

Fibres are also subject to orientational disorder. The polymer helices in noncrystalline fibres and the microcrystallites in crystalline fibres are not perfectly aligned to the fibre axis; the deviation from parallelism is called the disorientation of the fibre. Disorientation causes the reflections from crystalline fibres and the diffracted intensity from noncrystalline fibres to be spread into arcs (Debye–Scherrer arcs).

### 19.5.3. Diffraction by helical molecules

#### 19.5.3.1. Fibre diffraction patterns

As noted above, the diffraction pattern from a fibre is confined to layer lines because of the repeating nature of the polymer helix. The layer lines in reciprocal space are perpendicular to the fibre axis in real space. The layer line passing through the origin in reciprocal space is called the equator or zero layer line. The line in a diffraction pattern normal to the equator and passing through the origin is called the meridian. If the fibre axis is perpendicular to the incident X-ray beam, the recorded diffraction pattern is symmetric about both the equator and the meridian. If the fibre is not normal to the incident beam, the pattern is symmetric only about the meridian.

#### 19.5.3.2. Helical symmetry

It is convenient to use cylindrical coordinates to describe helical molecules. In real space we use coordinates  $(r, \varphi, z)$ ; in reciprocal space  $(R, \psi, Z)$ . By convention, the  $z$  axis is the helix axis and the line  $(\varphi = 0, z = 0)$  corresponds to the  $x$  axis in Cartesian coordinates. The repeat distance along the  $z$  axis is  $c$ . Within this distance, there are  $u$  repeating units in  $t$  turns of the helix. If the coordinates of a point in the first repeating unit are  $(r, \varphi, z)$ , then applying the helical symmetry gives the coordinates of the corresponding point in the  $(k+1)$ th repeating unit as  $(r, \varphi + 2\pi kt/u, z + kc/u)$ .

#### 19.5.3.3. Structure factors

Cochran *et al.* (1952) showed that the structure factor on layer line  $l$  of a helix made up of repeating subunits is

$$\mathbf{F}(R, \psi, Z) = \sum_j \sum_n f_j J_n(2\pi R r_j) \exp\{i[n(\psi + \pi/2) - n\varphi_j + 2\pi l z_j/c]\}. \quad (19.5.3.1)$$

Diffraction occurs only for  $Z = l/c$ .  $r_j, \varphi_j$  and  $z_j$  are the real-space coordinates of atom  $j$  in the repeating unit of the helix;  $f_j$  is the atomic scattering factor of that atom.  $J_n$  is the Bessel function of the first kind of order  $n$ . The summation over  $n$  includes only those values of  $n$  that satisfy the selection rule

$$l = tn + um, \quad (19.5.3.2)$$

where  $m$  is any integer. In practice, the summation may be limited to values of  $|n|$  less than  $2\pi r_{\max} R + 2$ , where  $r_{\max}$  is the radius of the outermost atom in the polymer, because the value of a Bessel function  $J_n(x)$  is negligible for  $n$  greater than about  $x + 2$ . For low-order Bessel functions or applications requiring greater accuracy, slight variations of this limitation are used.

The structure factor  $\mathbf{F}$  is a complex number with an amplitude and phase, and is fully equivalent to that derived using the trigonometric functions in crystallography. The expression for intensity  $I = \mathbf{F}\mathbf{F}^* = |\mathbf{F}|^2$  holds good.

Equation (19.5.3.1) can be rewritten (Klug *et al.*, 1958) as

$$\mathbf{F}(R, \psi, l/c) = \sum_n \mathbf{G}_{n,l}(R) \exp[in(\psi + \pi/2)], \quad (19.5.3.3)$$

where the Fourier–Bessel structure factor  $\mathbf{G}_{n,l}(R)$  is independent of  $\psi$  and is given by

$$\mathbf{G}_{n,l}(R) = \sum_j f_j J_n(2\pi R r_j) \exp[i(-n\varphi_j + 2\pi l z_j/c)]. \quad (19.5.3.4)$$

$J_n(0)$  is 1 when  $n = 0$  and 0 otherwise. For this reason, the structure factors on the meridian ( $R = 0$ ) are nonzero only on layer lines for which  $l$  is an integral multiple of  $u$ . Hence, a visual inspection of the diffraction pattern often helps to determine  $u$ .

#### 19.5.3.4. Fourier–Bessel syntheses

Electron densities may be calculated for crystalline fibres, as they are in crystallography, using Fourier syntheses with coefficients determined for the crystalline reflections.

For noncrystalline fibres, it is more convenient to use Fourier–Bessel syntheses: the electron density  $\rho$  at point  $(r, \varphi, z)$  is

$$\rho(r, \varphi, z) = (1/c) \sum_l \sum_n \mathbf{g}_{n,l}(r) \exp[i(n\varphi - 2\pi l z/c)], \quad (19.5.3.5)$$

where

$$\mathbf{g}_{n,l}(r) = \int_0^\infty \mathbf{G}_{n,l}(R) J_n(2\pi R r) 2\pi R \, dR. \quad (19.5.3.6)$$

#### 19.5.3.5. Diffracted intensities: noncrystalline fibres

The intensity in the diffraction pattern of a noncrystalline fibre is the cylindrical average of the square of the Fourier transform (Franklin & Klug, 1955):

$$\begin{aligned} I(R, l) &= \langle |\mathbf{F}(R, \psi, l/c)|^2 \rangle_\psi \\ &= \sum_n \mathbf{G}_{n,l}(R) \mathbf{G}_{n,l}^*(R) \\ &= \sum_n |\mathbf{G}_{n,l}(R)|^2. \end{aligned} \quad (19.5.3.7)$$

The intensity varies continuously as a function of  $R$  along each layer line (Fig. 19.5.2.1a).

#### 19.5.3.6. Diffracted intensities: polycrystalline fibres

The intensity in the diffraction pattern of a polycrystalline fibre consists of Bragg reflections on layer lines (Fig. 19.5.2.1b). On each layer line, owing to the lattice sampling that arises from the lateral organization of the polymers, intensities are observed at discrete  $R$  values defined by the reciprocal-lattice points. In the case of monoclinic (with  $c$  as the unique axis), orthorhombic and hexagonal systems, the reflection positions are determined by equations (19.5.3.8), (19.5.3.9) and (19.5.3.10), respectively.

$$R_{hk}^2 = h^2 a^{*2} + k^2 b^{*2} + 2hka^* b^* \cos \gamma^*, \quad (19.5.3.8)$$

$$R_{hk}^2 = h^2 a^{*2} + k^2 b^{*2}, \quad (19.5.3.9)$$

$$R_{hk}^2 = (h^2 + k^2 + hk) a^{*2}. \quad (19.5.3.10)$$

Consequently, on each layer line, superposition occurs between reciprocal-lattice points  $(hkl)$  and  $(\bar{h}\bar{k}l)$  for monoclinic;  $(hkl)$ ,  $(\bar{h}\bar{k}l)$ ,  $(h\bar{k}l)$  and  $(\bar{h}kl)$  for orthorhombic; and  $(hkl)$ ,  $(\bar{h}\bar{k}l)$ ,  $(khl)$ ,  $(\bar{k}\bar{h}l)$ ,  $(kil)$ ,  $(\bar{k}il)$ ,  $(ikl)$ ,  $(\bar{i}\bar{k}l)$ ,  $(ihl)$ ,  $(\bar{i}\bar{h}l)$ ,  $(hil)$  and  $(\bar{h}\bar{i}l)$ , where  $i = -(h+k)$ , for hexagonal systems. Depending upon the unit-cell dimensions, other reflections having the same  $R$  value may also be superposed to give a single intensity, and those having  $R$  values close to each other may be difficult to resolve. All superposed reflections must be